CONTRIBUTIONS to SCIENCE, **2** (2): 237-249 (2002)
Institut d'Estudis Catalans, Barcelona

focus

White dwarfs

Jordi Isern [1,2], Enrique García-Berro *[1,3], Margarida Hernanz [1,2] and Maurizio Salaris [4]

1 Institut d'Estudis Espacials de Catalunya, Barcelona

2 Institut de Ciències de l'Espai (CSIC), Barcelona

3 Departament de Física Aplicada, Universitat Politècnica de Catalunya, Barcelona

4 Astrophysics Research Institute, Liverpool John Moores University, Liverpool

White dwarfs are the final remnants of low and intermediate mass stars. Their evolution is essentially a cooling process that lasts for ≈10 Gyr and allows to obtain information about the age of the Galaxy as well as about the past history of the star formation rate in solar neighborhood. Therefore, it is important to identify all the relevant sources of energy as well as the mechanisms that control its flow to the space. In this paper we show the state of the art of the white dwarf cooling theory and the uncertainties still remaining. We also provide some applications of the theory of cooling white dwarfs to scrutiny the past history of the local star formation rate or the identification of objects responsible for the recently reported microlensing events to the obtention of tight upper limits to the rate of change of the gravitational constant or upper limits to the mass of the axion. Finally, future prospects in this field of astronomy are also reviewed.

1. Introduction

White dwarfs represent the last evolutionary stage of stars with masses smaller than 10±2 $M_\odot$, with the upper mass limit as yet unknown. Most of them are composed of carbon and oxygen, but white dwarfs with masses smaller than 0.4 $M_\odot$ are made of helium, while those more massive than ~1.05 $M_\odot$ are composed of oxygen and neon. The exact composition of the carbon-oxygen cores critically depends on evolution during the previous asymptotic giant branch phase. More specifically, it depends on the competition between the $^{12}C(\alpha,\gamma)^{16}O$ reaction and the triple-*a* rection, on the details of the stellar evolutionary codes and on the choice of several other nuclear cross sections. In a typical case, a white dwarf of 0.58 $M_\odot$, the total amount of oxygen represents 62% of the total mass while its concentration in the central layers of the white dwarf can be as high as 85%.

In all cases, the core is surrounded by a thin layer of pure helium with a mass in the range of 10^{-2} to 10^{-4} $M_\odot$. This layer is, in turn, surrounded by an even thinner layer of hydrogen with mass lying in the range of 10^{-4} to 10^{-15} $M_\odot$. This layer is missing in 25% of cases. From the phenomenological point of view, white dwarfs containing hydrogen are classified as DA while the remaining ones (the non-DA) are classified as DO, DB, DQ, DZ and DC, depending on their spectral features, and constitute a sequence of decreasing temperatures. The origin of these spectral differences and the relationship among them is as yet unelucidated although it is related to the initial conditions imposed by the evolution of AGB stars, the diffusion induced by gravity, thermal diffusion, radiative levitation, convection at the H-He and He-core interfaces, proton burning, stellar winds and mass accretion from the interstellar medium.

The structure of white dwarfs is sustained by the pressure of degenerate electrons and these stars are unable to obtain energy from thermonuclear reactions. Therefore, their evolution can be concisely described as a simple cooling process (Mestel, 1952) in which the internal degenerate core acts as a reservoir of energy and the outer non-degenerate layers control the energy outflow. If the core is assumed to be isothermal, which is justified by the high conductivity of degenerate electrons, and the envelope thin, then

$$L \approx -\frac{dU_{\rm th}}{dt} = -\overline{c_{\rm V}} M_{\rm WD} \frac{dT_c}{dt} \qquad (1)$$

$$\frac{L}{M_{\rm WD}} = f(T_{\rm c}) \qquad (2)$$

where $U_{\rm th}$ is the thermal content, $\overline{c_{\rm V}}$ is the average specific heat, $T_{\rm c}$ is the temperature of the (isothermal) core, and f ($T_{\rm c}$) is a function provided by the structure of the envelope that relates the core temperature to the star luminosity. All the remaining symbols have their usual meaning. A simple calculation indicates that the lifetime of these stars is very long, ~ 10 Gyr. They thus retain important information about the past history of the Galaxy. In particular, it is possible to obtain the stellar formation rate and the age of the different galactic components: disk, halo and globular clusters.

Moreover, the study of very cool white dwarfs bears important consequences, since the recent results of the microlensing experiments carried out by the MACHO team (Alcock et al., 1997) show that perhaps a substantial fraction of the halo of dark matter could be in the form of very cool white

* Author for correspondence: Enrique García-Berro, Departament de Física Aplicada, Universitat Politècnica de Catalunya. Campus Nord, Edifici B-4. Jordi Girona, 1-3. 08034 Barcelona. Catalonia (Spain). Tel. 34 934016898. Fax: 34 934016090. Email: garcia@fa.upc.es

dwarfs. The search for these elusive white dwarfs has been unsuccessful to date, although there are signs that perhaps the observational counterparts of these white dwarfs could be the stellar objects recently reported in the Hubble Deep Field (Ibata et al., 1999; Méndez and Minniti, 2000).

The structural simplicity of white dwarfs also makes them ideal laboratories for testing new physics since any perturbation of the cooling rate inmediately translates into a perturbation of the luminosity function or of the secular variation of the period of pulsation of variable white dwarfs. For instance, Isern et al. (1992) used ZZ Ceti stars (a class of pulsating white dwarfs) to constrain the mass of the axions (Isern et al., 1992), whereas Blinnikov and Dunina-Barkovskaya (1994) used the properties of hot white dwarfs to constrain the magnetic momentum of the neutrino, and García-Berro et al. (1995) used the distribution of the coldest white dwarfs to bound any possible variation of the gravitational constant, G.

The influence of Coulomb interactions on specific heat was early recognized by Kirshnitz (1960), Abrikosov (1960) and Salpeter (1961). This idea led (Van Horn, 1968; Lamb and Van Horn, 1975), in a natural way, to considering the influence of crystallization, and the subsequent release of latent heat, on white dwarf evolution. Later, Stevenson (1980) and Mochkovitch (1983) examined the release of gravitational energy associated with the change of the chemical composition induced by crystallization in C/O mixtures. Finally, Isern et al. (1991) examined the consequences of the deposition of ^{22}Ne, the most abundant of the impurities present in a white dwarf, in the central regions, and Xu and Van Horn (1992) made the same calculation for ^{56}Fe, the second impurity in importance.

It is clear that white dwarfs can not only provide information about the Galaxy, but they can also be considered excellent laboratories to study the behavior of matter under extreme conditions. Furthermore, the simplicity of their structure and evolution makes them extremely useful as astroparticle physics laboratories. But such studies require good observational background, good evolutionary models and good input physics. In this paper we will examine the relevance of these factors.

2. The evolution of white dwarf envelopes

As mentioned above, the envelope of white dwarf stars is a very thin layer ($M_e < 10^{-2}\, M_\odot$), partially degenerate, partially or totally ionized and sometimes convective. The envelope completely controls the emergent flux of energy. Its behavior is the result of:

1. A non-standard initial chemical composition resulting from hydrogen and helium shell burning in AGB stars,
2. a very efficient gravitational settling that induces the stratification of the envelope in almost chemically pure layers with the lightest element at the top (Schatzman, 1958), and
3. the existence of mechanisms tending to restore homogeneity, like convective mixing (D'Antona and Mazzitelli, 1978; Fontaine et al., 1984; Pelletier et al., 1986; MacDonald, Hernanz and José, 1998), radiative levitation (Fontaine and Michaud, 1979; Vauclair, Vauclair and Greenstein, 1979), thermal diffusion (Schatzman, 1958), accretion from the interstellar medium (Alcock and Illarionov, 1980), winds and so on.

There is now a broad opinion that the distinction between DA and non-DA character is inherited (i.e. linked to the origin of the white dwarf itself) although a fraction of white dwarfs can change their external aspect during evolution (Shipman, 1997). Standard evolution theory predicts that typical field white dwarfs have a core mass in the range of 0.5 to 1.0 $M_\odot$ made up of a mixture of carbon and oxygen surrounded by a helium mantle of $M_{He} \simeq 10^{-2}\, M_{WD}$, itself surrounded by a hydrogen envelope of $M_H \simeq 10^{-4}\, M_{WD}$ (Iben and Tutukov, 1984; Koester and Schönberner, 1986; D'Antona and Mazzitelli, 1978). Adjusting the parameters in the AGB models it is possible in 25% of cases to obtain a white dwarf totally devoid of the hydrogen layer. Since the relative number of DA/non-DA stars changes as evolution proceeds, a mechanism capable of changing this property must exist (Shipman, 1997; Fontaine and Wesemael, 1997).

The idea is that DA white dwarfs start as a central star of a planetary nebula. When its temperature is high enough ($T_{eff} >$ 40,000 K) radiative levitation brings metals to the photosphere and heavy element lines appear in its spectrum. As the temperature goes down, these elements settle down and disappear. When DAs arrive at the instability phase strip they pulsate as ZZ Ceti stars. Pulsational data indicate that the masses of the hydrogen layer are in the range of 10^{-8} – $10^{-4}\, M_\odot$ thus indicating that DAs are born with a variety of layer masses. As the DA star cools down, the convection zone deepens and, depending on the mass, reaches the helium layer. When this happens, helium is dredged up and the DA white dwarf turns into a non-DA. Consequently, the ratio between the number of DAs and non-DAs decreases. Stars with a thin H layer ($<10^{-9}\, M_\odot$) mix at high temperatures while those having a thick layer ($\sim 10^{-4}\, M_\odot$) never do so .

The evolution of a non-DA star is more complex. These are born as He-rich central stars of planetary nebulae and, as they cool down, they become first PG 1159 stars and then DO stars. The trace amounts of hydrogen still present in the helium envelope gradually float up to the surface and when the effective temperature is of the order of 50,000 K the outer H layer becomes thick enough to conceal the He layer and to convert the star into a DA star. When the temperature drops below 30,000 K, the helium convection zone increases and hydrogen is engulfed and mixed within the helium layer once more. The white dwarf is observed as a non-DA, more precisely as a DB. This lack of non-DA stars in the temperature range of 30,000 to 45,000 K is known as the DB gap. The DB stars gradually cool down and become DZ and DC stars (a fraction of them being DAs in origin). Due to the convective dredge up at the bottom of the helium envelope,

some of the non-DAs show carbon in their spectra (DQ stars). Because of accretion from the interstellar medium some of them show hydrogen lines in their spectra (they are known as DBA class).

3. Overview of white dwarf evolution

The evolution of white dwarfs from the planetary nebula phase to its disappearance depends on the properties of the envelope and the core and has been discussed in detail by Iben and Tutukov (1984), Koester and Schönberner (1986), D'Antona and Mazzitelli (1989), and Isern et al. (1998a). To summarize, the cooling process can be roughly divided into four stages: neutrino cooling, fluid cooling, crystallization and Debye cooling.

- Neutrino cooling: $\log(L/L_\odot) > -1.5$. This stage is very complicated because of the dependence on the initial conditions of the star as well as on the complex and not yet well understood behavior of the envelope. For instance, Iben and Tutukov (1984) found that the luminosity due to hydrogen burning through the pp chains would never stop and could become dominant at relatively low luminosities, $-3.5 \leq \log (L/L_\odot) \leq -1.5$. It is worth noting that, if this were the case, the cooling rate would be similar to the normal one (i.e., the one that this source neglects) and it would be observationally impossible to distinguish between both possibilities. However, the importance of such a source strongly depends on the mass, M_H, of the hydrogen layer. If $M_H \leq 10^{-4}\ M_\odot$, the pp contribution quickly drops and never becomes dominant. Since astero-seismological observations seem to constrain the size of M_H well below this critical value, this source can be neglected. Fortunately, when neutrino emission becomes dominant, the different thermal structures converge to a unique one, assuring uniformity of the models with $\log(L/L_\odot) \leq -1.5$. Furthermore, since the time necessary to reach this value is $\leq 8 \times 10^7$ years (D'Antona and Mazzitelli, 1989) for any model, its influence on total cooling time is negligible.
- Fluid cooling: $-1.5 \geq \log (L/L_\odot) \geq -3$ The main source of energy is the gravothermal one. Since the plasma is not very strongly coupled ($\Gamma < 179$), its properties are reasonably well known (Ségretain et al., 1994). Furthermore, the flux of energy through the envelope is controlled by a thick nondegenerate layer with an opacity dominated by hydrogen (if present) and helium, and weakly dependent on the metal content. The main source of uncertainty is related to the chemical structure of the interior, which depends on the adopted rate of the $^{12}C(\alpha,\gamma)^{16}O$ reaction and on the treatment given to semi-convection and overshooting. If this rate is high, the oxygen abundance is higher in the center than in the outer layers, resulting thus in a reduction of the specific heat at the central layers where the oxygen abundance can reach values as high as $X_O = 0.85$ (Salaris et al., 1997).
- Crystallization: $\log (L/L_\odot) < -3$. Crystallization introduces two new sources of energy: latent heat and sedimentation. In the case of Coulomb plasmas, the latent heat is small, of the order of $k_B T_s$ per nuclei, where k_B is the Boltzmann constant and T_s is the temperature of solidification. Its contribution to the total luminosity is small, ~ 5%, but not negligible (Shaviv and Kovetz, 1976).

  During the crystallization process, the equilibrium chemical compositions of the solid and liquid plasmas are not equal. Therefore, if the resulting solid flakes are denser than the liquid mixture, they sink towards the central region. If they are lighter, they rise upwards and melt when the solidification temperature, which depends on the density, becomes equal to that of the isothermal core. The net effect is a migration of the heavier elements towards the central regions with the subsequent release of gravitational energy (Mochkovitch, 1983). Of course, the efficiency of the process depends on the detailed chemical composition and on the initial chemical profile and it is maximum for a half oxygen-half carbon mixture uniformly distributed throughout the star.
- Debye cooling: When practically the entire star has solidified, the specific heat follows Debye's law. However, the outer layers still have very large temperatures as compared with Debye's temperature, and since their total heat capacity is still large enough, they prevent the sudden disappearance of the white dwarf in the case, at least, of thick envelopes (D'Antona and Mazzitelli, 1989).

4. The physics of crystallization

4.1 The carbon-oxygen mixture

The first calculation of a phase diagram for C/O mixtures was made by Stevenson (1980) who obtained a eutectic shape. This result was a consequence of his assumption that the solid was entirely random. Under this assumption the free energy was given by $F \sim -0.9\ \Gamma$, with $\Gamma = \overline{Z}^{5/3}\ \Gamma_e$, where $\overline{Z} = \sum Z_i x_i$ and x_i is the abundance by number. Since the mixture retains some short range order, the free energy is then given by the linear mixing rule,

$$F_{lm} \approx -0.9 \overline{Z}^{5/3} \Gamma_e ,$$

as was proved later. Therefore, the solid phase was less stable, and thus $F > F_{lm}$, consequently resulting in eutectic behavior of the phase diagram.

Barrat et al. (1988) used the density functional theory of freezing and the mean spherical approximation, but with the same diameter for the two chemical species, to compute the correlation between the particles. As a consequence they obtained a phase diagram of the spindle form. Moreover, they used the value $\Gamma_C = 168$ for the crystallization of the

pure phase. Ichimaru et al. (1988) performed a similar calculation in the framework of the density functional theory but using the Improved Hypernetted Chain approximation to compute the correlation functions. They found an azeotropic phase diagram with an azeotropic concentration of carbon $x_C = 0.16$. Finally, Ségretain and Chabrier (1993) extended the calculations of Barrat et al. (1988) considering the effects of the different diameters of the two chemical species and essentially found the same results as Barrat et al. (1988). It is interesting to notice here that for the astrophysical applications and the usual abundances of carbon and oxygen found in white dwarf interiors the three phase diagrams lead to the same results when all of them employ the same value $\Gamma_C = 180$ for the Coulomb coupling parameter at crystallization.

Because of the spindle shape of the phase diagram of C/O mixtures, the solid formed upon crystallization is richer in oxygen than the liquid and therefore denser. The density excess can be estimated using the condition of pressure continuity as:

$$\frac{\delta\rho}{\rho} \approx -\frac{\delta P_{\rm i}}{\gamma P_{\rm e}} - \frac{\delta Y_e}{Y_e} \tag{3}$$

where $P_{\rm i}$ and $P_{\rm e}$ are the ionic and electronic pressures respectively, γ is the electron adiabatic index and $Y_{\rm e}$ is the number of electrons per nucleon. For a 0.6 $M_\odot$ white dwarf with equal amounts of carbon and oxygen, $\delta\rho/\rho \sim 10^{-4}$. Therefore the solid settles down at the core of the star and the lighter liquid left behind is redistributed by Rayleigh-Taylor instabilities (Stevenson, 1980; Mochkovitch, 1983). The result is an enrichment of oxygen in the central layers and its depletion in the outer ones.

Since the efficiency of convective mixing is very high (Isern et al., 1997; Mochkovitch et al. 1997) the gradient of the carbon mass fraction is given by:

$$\left|\frac{dX_{\rm C}}{dr}\right| \cong 4{\rm x}10^{-12}\left(\frac{v_{\rm crys}}{0.1{\rm cm/yr}}\right)\left(\frac{\Delta X_{\rm C}}{0.1}\right)\left(\frac{100{\rm cm}^2 s^{-1}}{K_T}\right)\left(\frac{1}{\rm P}\right) \tag{4}$$

where $v_{\rm crys}$ is the velocity of the crystallization front (~ 0.1 cm yr^{-1}), K_T is the thermal conductivity, P is the Peclet number, given by $P = \tau_{\rm cond}/\tau_{\rm conv}$, where $\tau_{\rm cond} = l^2/K_T$ is the time scale for thermal conduction and $\tau_{\rm conv} = l/\upsilon_{\rm conv}$ is the convective turn-over time scale, l the mixing length $\upsilon_{\rm conv}$ being the velocity of the convective eddies. For the typical conditions of white dwarf interiors the gradient is so small that X_C varies by less than 1% in the convective region, and the the liquid phase can be considered well mixed (see Isern et al., 1997; and Mochkovitch et al., 1997 for more details).

With the hypothesis of perfect mixing, the composition profile can be easily computed. Consider a partially solidified white dwarf of total mass $M_{\rm WD}$ containing a total amount of oxygen $M_{\rm O}$. Its structure can be divided into three parts: a solid core of mass $M_{\rm S}$ and oxygen mass fraction $X_{\rm S}$ (m), a liquid mantle of mass ΔM homogenized by convection, with oxygen abundance X, and an outer, unperturbed region, with the initial oxygen profile $X_{\rm O}$ (m). Therefore, the total mass of oxygen can be written as

$$M_{\rm O} = \int_0^{M_{\rm S}} X_{\rm S} dm + X(M_{\rm L} - M_{\rm S}) + \int_{M_{\rm L}}^{M_{\rm WD}} X_{\rm O}\, dm \tag{5}$$

where $M_{\rm L} = M_{\rm S} + \Delta M$

After deriving this expression with respect to the solid mass and introducing the two conditions $X_{\rm S}(M_{\rm S}) = (1+\alpha)X$ and $X = X_{\rm O}(M_{\rm S})$, where α, which depends on X, is the degree of enrichment produced during crystallization, we obtain:

$$\alpha X + \frac{dX}{dM_{\rm S}}\left(M_{\rm L} - M_{\rm S}\right) = 0 \tag{6}$$

introducing $q = M_{\rm S}/M_{\rm WD}$ and $q_{\rm L} = M_{\rm L}/M_{\rm WD}$,

$$\frac{dX}{dq}\left[q_{\rm L}(X) - q\right] + \alpha(X)X = 0 \tag{7}$$

Notice the singularity at $q = 0$ since $q_{\rm L}(X) = 0$ and also notice that if the initial profile is flat, $q_{\rm L}(X) = 1$. Integration of this equation provides the final oxygen profile after crystallization (Salaris et al., 1997).

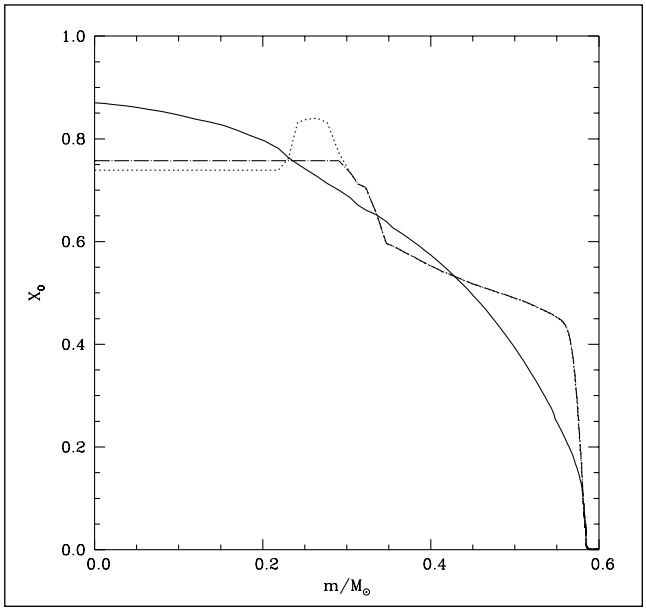

Figure 1. Oxygen profile of a 0.61 $M_\odot$ white dwarf at the beginning of the thermally-pulsing AGB phase (dotted line), the same after rehomogenization by Rayleigh-Taylor instabilities during the liquid phase (dotted-dashed line) and after total freezing (solid line)

Figure 1 displays the oxygen profiles for the CO core of a ~ 0.6 $M_\odot$ white dwarf progenitor obtained just at the end of the first thermal pulse (dotted line). The inner part of the core, with a constant abundance of ^{16}O, is determined by the maximum extension of the central He-burning convective region while the peak in the oxygen abundance is produced when the He-burning shell crosses the semiconvective region partially enriched in ^{12}C and ^{16}O, and carbon is converted into oxygen through the $^{12}C(\alpha,\gamma)^{16}O$ reaction. Beyond this region, the oxygen profile is built when the thick He-burning shell is moving towards the surface. Simultaneously, gravitational contraction increases its temperature and density, and since the ratio between the $^{12}C(\alpha,\gamma)^{16}O$ and 3α reaction rates is lower for larger temperatures the oxygen mass fraction steadily decreases in the external part of the C/O core.

The ^{12}C and ^{16}O profiles at the end of the first thermal pulse have an off-centered peak in the oxygen profile, which is related to semiconvection. Since Salaris et al. (1997) chose the rate of Caughlan et al. (1985) for the $^{12}C(\alpha,\gamma)^{16}O$ reaction, they were forced to use the Scwarzschild criterion for convection and, therefore, they did not find the chemical profiles to be Rayleigh-Taylor unstable during the early thermally-pulsing AGB phase. After ejection of the envelope, when the nuclear reactions are negligible at the degenerate core, the Ledoux criterion can be used and, therefore, the chemical profiles are Rayleigh-Taylor unstable and, consequently, are rehomogeneized by convection. We observe that, in any case, this rehomogeneization minimizes the effect of the separation occurring during the cooling process. Figure 1 also shows the the resulting oxygen profile after rehomogeneization (dotted-dashed line), and the oxygen profile after complete crystallization (solid line).

4.2 The role of minor species

As already mentioned, the ^{22}Ne isotope is the most abundant impurity in white dwarfs. Its abundance is directly related to the initial abundances of CNO elements, which, after the H-burning phase become ^{14}N. This isotope, in turn, becomes ^{22}Ne after the series of reactions $^{14}N(\alpha,\gamma)^{18}O(\alpha,\gamma)^{22}Ne$, during the He-burning phase. Because of its high neutron number and the high sensitivity of degenerate structures to the electron number profile, ^{22}Ne can induce a large release of gravitational energy if, as a consequence of crystallization, it migrates towards the center during crystallization (Isern et al., 1991). For stars of solar metallicity, the typical abundances are 1-2%. A similar effect can be produced by the deposition of ^{56}Fe at the center (Xu and Van Horn 1992). Typical abundances are in this case 0.1%.

The physics of the deposition of the minor species is intricate since it depends on the behavior of a multicomponent diagram that is not known. A first step consists in assuming that the C/O/Ne or C/O/Fe mixtures behave as an effective binary mixture composed by neon (or iron) and an average element, representative of the C/O mixture.

Ségretain and Chabrier (1993) also computed the crystallization diagram for arbitrary ionic mixtures as a function of the charge ratio and found that the phase diagram was of the spindle form for $0.72 < Z_1/Z_2 < 1$, of the azeotropic form for $0.58 < Z_1/Z_2 < 0.72$ and of the eutectic form for $Z_1/Z_2 < 0.58$. In the case of a C/O mixture made of half and half of species, the resulting average element has such a charge that the corresponding phase diagram shows an azeotropic behavior with an azeotropic abundance of $X_a = 0.16$, which means that white dwarfs are on the neon poor side of the phase diagram. As a consequence, the solid in equilibrium with the liquid has a smaller concentration of neon and, since it is lighter than the surrounding liquid, it will rise and melt in lower density regions so that the neon concentration in the liquid will increase more and more until it reaches the azeotropic composition. This process of "distillation" will continue until all ^{22}Ne is collected in a central sphere of mass $M_W \times X_0(Ne)/X_a(Ne)$.

Ségretain (1996) computed a preliminary ternary diagram that displays the expected behavior at the binary limit (spindle form for the C/O mixture, azeotropic form for the C/Ne mixture and spindle form for the O/Ne mixture). For small concentrations of neon, and temperatures well above the azeotropic temperature, the crystallization diagram is not afected by the presence of neon. However, as the azeotropic temperature is approached, the resulting solid is lighter than the surrounding liquid and the distillation process starts as in the previous case. The main difference is that it starts in the outer layers instead of the central layers and the effect of separation is therefore a good deal smaller.

5. The energetics of the cooling process

The local energy budget of the white dwarf can be written as:

$$\frac{dL_\Gamma}{dm} = -\varepsilon_\upsilon - P\frac{dV}{dt} - \frac{dE}{dt} \tag{8}$$

where all the symbols have their usual meaning. If the white dwarf is made of two chemical species with atomic numbers Z_0 and Z_1, mass numbers A_0 and A_1, and abundances by mass X_0 and X_1, respectively ($X_0 + X_1 = 1$), where the suffix 0 refers to the heavier component, this equation can be written as:

$$-\left(\frac{dL_\Gamma}{dm} + \varepsilon_\upsilon\right) = C_V\frac{dT}{dt} + T\left(\frac{\partial P}{\partial T}\right)_{V,X_0}\frac{dV}{dt} - l_s \cdot \frac{dM_S}{dt}\delta(m - M_S) + \left(\frac{\partial E}{\partial X_0}\right)_{T,V}\frac{X_0}{dt} \tag{9}$$

where l_S is the latent heat of crystallization and M_s is the rate at which the solid core grows; the delta function indicates that the latent heat is released at the solidification front. Notice that chemical differentiation contributes to the luminosity not only through compressional work, which is negligible, but also through the change in the chemical abundances,

which leads to the last term of this equation. Notice, as well, that the largest contribution to L_r due to the change in E exactly cancels out the PdV work for *any* evolutionary change (with or without a compositional change). This is, of course, a well known result (Mestel, 1952; Shaviv and Kovetz, 1976; Lamb and Van Horn, 1975; D'Antona and Mazzitelli, 1990) that can be related to the release of gravitational energy (Isern et al., 1997).

Integrating over the whole star, we obtain:

$$L + L_\nu = -\int_0^{M_{\rm WD}} C_{\rm V} \frac{dT}{dt} dm - \int_0^{M_{\rm WD}} T \left(\frac{\partial P}{\partial T}\right)_{\rm V,X_0} \frac{dV}{dt} dm + l_{\rm s} \frac{dM_{\rm S}}{dt} - \int_0^{M_{\rm WD}} \left(\frac{\partial E}{\partial X_0}\right)_{T,V} \frac{dX_0}{dt} dm \qquad (10)$$

The first term of the equation is the wellknown contribution of the heat capacity of the star to the total luminosity (Mestel, 1952). The second term represents the contribution to the luminosity due to the change of volume. It is in general small since only the thermal part of the electronic pressure, the ideal part of the ions and the Coulomb terms other than the Madelung term contribute (Shaviv and Kovetz, 1976; Lamb and Van Horn, 1975). However, when the white dwarf enters into the Debye regime, this term provides about 80% of the total luminosity preventing the sudden disappearence of the star (D'Antona and Mazzitelli, 1990). The third term represents the contribution of the latent heat to the total luminosity at freezing. Since the latent heat of Coulomb plasmas is small its contribution to the total luminosity is modest although not negligible. The fourth term represents the energy released by the chemical readjustment of the white dwarf, i.e., the release of the energy stored in the form of chemical potentials. This term is usually negligible in normal stars, since it is much smaller than the energy released by nuclear reactions, but it must be taken into account when all other energy sources are small.

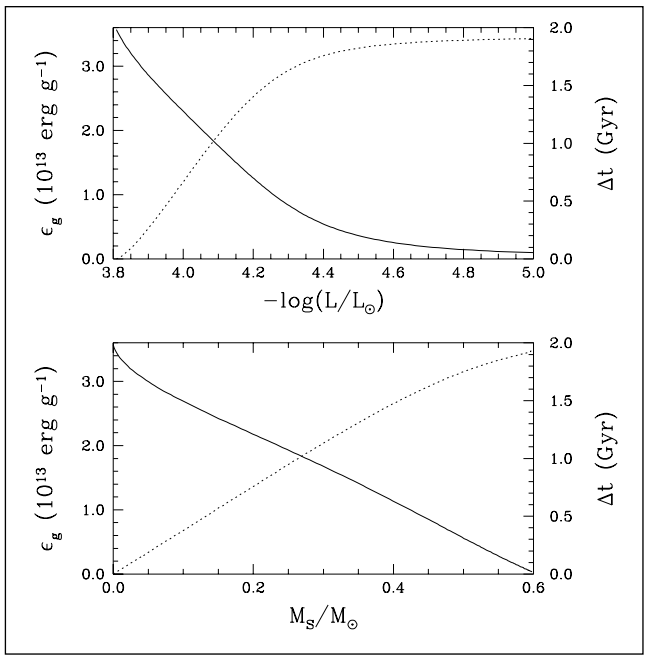

Figure 2. Energy released by the redistribution of elements per unit of crystallized mass (continuous line) and the corresponding time delay in the cooling (dotted line) as a function of the solid mass (lower panel) and the luminosity (upper panel)

The last term can be further expanded and written as (Isern et al., 1997):

$$\int_0^{M_{\rm WD}} \left(\frac{\partial E}{\partial X_0}\right)_{T,V} \frac{dX_0}{dt} dm = \left(X_0^{\rm sol} - X_0^{\rm liq}\right) \left[\left(\frac{\partial E}{\partial X_0}\right)_{M_{\rm S}} - \left\langle \frac{\partial E}{\partial X_0} \right\rangle\right] \frac{dM_{\rm S}}{dt} \qquad (11)$$

where

$$\left\langle \frac{\partial E}{\partial X_0} \right\rangle = \frac{1}{\Delta M} \int_{\Delta M} \left(\frac{\partial E}{\partial X_0}\right)_{T,V} dm \qquad (12)$$

and it is possible to define the total energy released per gram of crystallized matter as:

$$\epsilon_{\rm g} = -\left(X_0^{\rm sol} - X_0^{\rm liq}\right) \left[\left(\frac{\partial E}{\partial X_0}\right)_{M_{\rm S}} - \left\langle \frac{\partial E}{\partial X_0} \right\rangle\right] \qquad (13)$$

The square bracket is negative since $(\partial E / \partial X_0)$ is negative and essentially depends on the density, which monotonically decreases outwards.

The delay introduced by solidification can be easily estimated to a good approximation if it is assumed that the luminosity of the white dwarf is just a function of the temperature of the nearly isothermal core (Isern et al. 1997). In this case:

$$\left\langle \frac{\partial E}{\partial X_0} \right\rangle = \frac{1}{\Delta M} \int_{\Delta M} \left(\frac{\partial E}{\partial X_0}\right)_{T,V} dm \qquad (14)$$

where $\epsilon_{\rm g}$ is is the energy released per unit of crystallized mass and $T_{\rm c}$ is the temperature of the core when the crystallization front is located at m. Of course, the total delay essentially depends on the transparency of the envelope. Any change in one sense or another can amplify or damp the influence of solidification and for the moment no reliable envelope models exist at low luminosities.

Table 1 displays the energy released in an otherwise typical, 0.6 $M_\odot$ white dwarf and the delays introduced by the different cases of solidification discussed here assuming that the envelope is the same as in Isern et al. (1997) and Ségretain et al. (1994) and that the white dwarf is made of half carbon and half oxygen. The symbol A represents the effective binary mixture. Its use is probably justified in the case of impurities of very high number such as iron. However, in the case of Ne this assumption is most probably doubtful as shown by Ségretain (1996).

Table 1. Energy released by the chemical differentiation induced by crystallization and the corresponding delays.

Mixture	ΔE*(erg)*	Δt *(Gyr)*
C/O	1.95×10^{46}	1.81
A/Ne	1.52×10^{47}	9.09
A/Fe	2.00×10^{46}	1.09
C/O/Ne	0.20×10^{46}	0.60

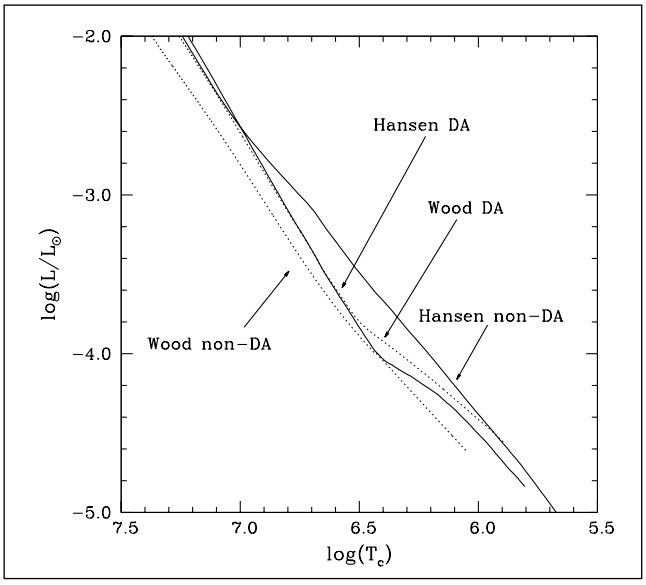

Figure 3. The relationships between the core temperature and the luminosity for various model atmospheres, see text for details.

Figure 2 displays the evolution of the energy released per unit mass crystallized as the solidification proceeds. The energy released near the center of the white dwarf is ε_g=3.54 x 10^{13} erg/g and the partial contribution of electrons and ions are, respectively ε_e= –5.00 x 10^{12} erg/g and ε_i= 4.04 x 10^{13} erg/g. The electron term is negative and different from zero only due to the mass defect of oxygen (A_0 = 16 – 3.18 x 10^{-4}) relative to carbon. If we had considered other species with a higher number of neutrons as compared with protons, as is the case of ^{22}Ne or ^{56}Fe, the situation would have been the reverse. The total energy released during this process is 1.95 x 10^{46} erg.

As previously stated, the total delay depends on the transparency of the envelope. In order to illustrate the effects of the transparency of the envelope in the cooling times, in Figure 3 we show several different core temperature-luminosity relationships. The first model atmosphere was obtained from the DA model sequence of Wood (1995), which has a mass fraction of the helium layer of q_{He} = 10^{-4} and a hydrogen layer of q_H =10^{-2}; the second model atmosphere is the non-DA model sequence of Wood and Winget (1989) which has a helium layer of q_{He} = 10^{-4} . However, it should be noted that between these two model sequences there was a substantial change in the opacities, and therefore the comparison is meaningless (i.e., the non-DA model is more opaque than the DA one). The remaining two model atmospheres are those of Hansen (1999) for both DA and non-DA white dwarfs. These atmospheres have been computed with state of the art physical inputs for both the equation of state and the opacities for the range of densities and temperatures relevant for white dwarf envelopes (although it should be mentioned that the contributions to the opacity of H^{3+} and H^{2+} ions were neglected in this calculation) and have the same hydrogen and helium layer mass fractions as those of Wood (1995) and Wood and Winget (1989), respectively. In all cases, white dwarf mass is 0.606 $M_\odot$ and the initial chemical profile of the C/O mixture is that of Salaris et al. (1997).

From figure 3 one can clearly see that the DA model atmospheres of Wood (1995) and Hansen (1999) are in very good agreement down to temperatures of the order of $\log(T_c) \approx 6.5$, whereas at lower temperatures the model atmospheres of Hansen (1999) predict significantly lower luminosities (that is, they are less transparent). This is undoubtedly due to the significant improvement in cool white dwarf atmosphere calculations in Hansen (1999). In contrast, Hansen's (1999) non-DA model atmosphere is by far more transparent at any temperature than the corresponding model of Wood and Winget (1989). This is clearly due to the fact that the Wood and Winget (1989) $L(T_c)$ relation was based on the old Los Alamos opacities which include a finite contribution from metals whereas Hansen (1999) non-DA atmospheres are made of pure helium.

With these two sets of model atmospheres Isern et al. (2000) computed cooling sequences for the following two cases: 1) crystallization and no phase separation and 2) crystallization and phase separation. The results are shown in Figure 4. The left panel of Figure 4 shows the cooling sequences for the non-DA model envelopes of Hansen (1999) – solid lines – and Wood and Winget (1989) – dotted lines. The sequences with phase separation correspond, obviously, to the cooling curves with larger cooling times for the same luminosity. The right panel of Figure 4 shows the same

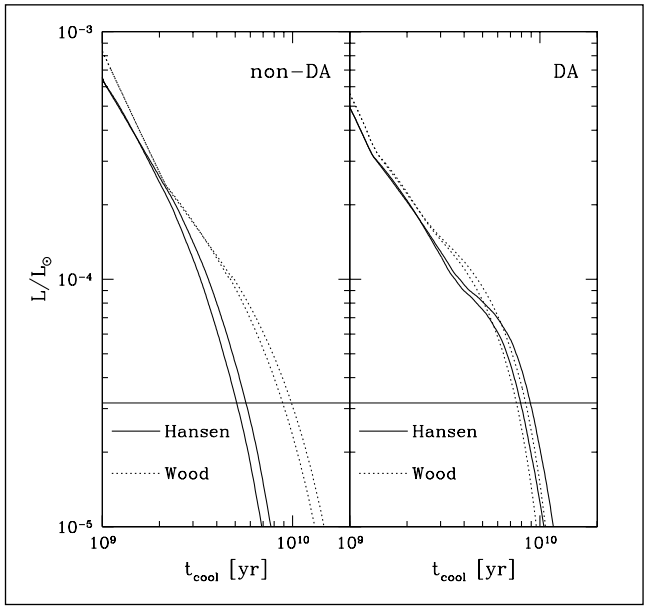

Figure 4. Cooling curves (time is in yr) for the white dwarf models described in the text, the thinner horizontal line corresponds to $\log(L/L_\odot)$= – 4.5, which is the approximate position of the observed cut-off of the white dwarf luminosity function.

Table 2. Uncertainties in the estimates of the cooling time of white dwarfs

Input	Δt *(Gyr)*	*Comments*
DA/non–DA	< 3.0	Very uncertain
Core composition	< 0.5	Depending on the $^{12}C(\alpha, \gamma)\ ^{16}O$
Opacity	< 0.4	
Metals in the envelope	≈ 0.2	
Additive contributions of the crystallization process		
C / O	0.8–1.2	Depending on the $^{12}C(\alpha, \gamma)\ ^{16}O$
Fe	< 1.3	
Ne	< 9.0	Binary mixture
	< 0.5	Ternary mixture
Observational	1–2	

set of calculations for the hydrogen-dominated white dwarf envelopes described previously. Clearly the cooling times are very different depending on the assumed physical characteristics of the adopted atmosphere.

Table 2 displays the uncertainties in the time necessary to fade until $\log(L/L_\odot) = -4.5$. In the lower section of this table the additive contributions to the uncertainty due to the physics of crystallization are shown, whereas the upper section describes the uncertainties due to the rest of the input physics. As can be seen, the major contribution is provided by the minor chemical species.

6. The age and the properties of the Galactic disk and halo

The white dwarf luminosity function is defined as the number of white dwarfs with bolometric magnitude $M_{\rm bol}$ per cubic parsec and unit bolometric magnitude. The first luminosity functions were obtained by Weidemann (1968), Kovetz and Shaviv (1976) and by Sion and Liebert (1977). Later on, Fleming et al. (1986) largely improved this function in the domain of white dwarfs brighter than $\log(L/L_\odot) \approx -3.3$, while Liebert et al. (1988) did the same for the coolest ones. Since then, the luminosity function of disk white dwarfs has received considerable attention both from the theoretical point of view (García-Berro et al., 1988a and b; Yuan, 1989; Hernanz et al., 1994; García-Berro et al., 1996; Wood and Oswalt, 1998; García-Berro et al., 1999) and the observational point of view (Oswalt et al., 1996; Leggett et al., 1998; Knox et al., 1999). The two main properties of this empirical luminosity function are its monotonic increase when the luminosity decreases, which indicates the cooling nature of the evolution of white dwarfs, and the existence of a short fall at $\log(L/L_\odot) \approx -4.5$ which is interpreted as a consequence of the finite age of the Galaxy. From the comparison between this empirical function and the theoretical one, it is possible to obtain the age of the disk, T, and the star formation rate, $\Psi(t)$, as a function of time (Díaz-Pinto et al., 1994).

Regarding the luminosity function of halo white dwarfs very lilttle can be said due to the lack of observational data. However, there have been considerable efforts to improve the current situation, the most noticeable ones being those of Liebert et al. (1989) and Torres et al. (1998). Similarly, and from a purely theoretical point of view, there have also been calculations that reproduce reasonably well the scarce observational data (Mochkovitch et al., 1990; Tamanaha et al., 1990; Isern et al., 1998). Hopefully, future missions like GAIA will remedy this situation (Figueras et al., 1999).

The luminosity function can be computed as

$$\propto \int_{M_{\rm i}}^{M_{\rm S}} \Phi(M)\Psi(T - t_{\rm cool}(l, M) - t_{\rm MS}(M))\tau_{\rm cool}$$

$$(l, M)dM \qquad (15)$$

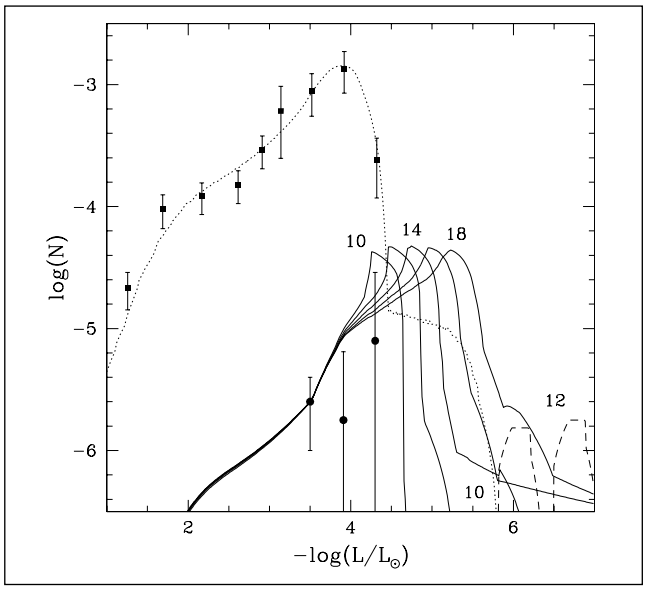

Figure 5. Luminosity functions of disk and halo white dwarfs as a function of the luminosity

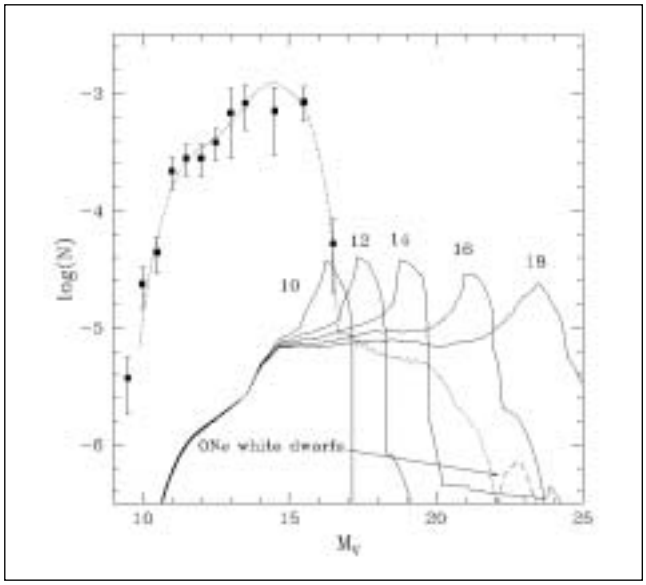

Figure 6. Luminosity functions of disk and halo white dwarfs as a function of the visual magnitude

where l is the logarithm of the luminosity in solar units, M is the mass of the parent star (for convenience all white dwarfs are labelled with the mass of the main sequence progenitor), t_{cool} is the cooling time down to luminosity l, $\tau_{cool} = dt/dM_{bol}$ is the characteristic cooling time, M_s and M_i are the maximum and the minimum masses of the main sequence stars able to produce a white dwarf of luminosity l, t_{MS} is the main sequence lifetime of the progenitor of the white dwarf, and T is the age of the population under study. The remaining quantities, the initial mass function, $\Phi(M)$, and the star formation rate, $\Psi(t)$, are not known a priori and depend on the astronomical properties of the stellar population under study.

Proper comparison of the observations requires one to bin this function in intervals of magnitude ΔM_{bol}, usually unit or half magnitudes, in the following way:

$$\left\langle n(l)\right\rangle_{\Delta l} = \frac{1}{\Delta l}\int_{-0.5\Delta l}^{+0.5\Delta l} n(l)dl \qquad (16)$$

where Δl is the size of the luminosity bin that corresponds to ΔM_{bol}. It is important to notice here that this binning procedure smooths and ultimately erases the spikes introduced by the sedimentation of Ne and Fe in the observational luminosity function. Therefore, in order to observationally detect the influence of these impurities, high resolution luminosity functions would be required.

Figures 5 and 6 display the luminosity functions of halo and disk white dwarfs computed with a standard initial mass function (Salpeter 1955). The adopted cooling sequences were from Salaris et al. (1997), which do not include the effects of Ne and Fe. The observational data for both the disk and the halo were taken from Liebert et al. (1988, 1989). The theoretical luminosity functions were normalized to the points $\log(L/L_\odot) \sim -3.5$ and $\log(L/L_\odot) \sim -2.9$ for the halo and the disk respectively due to their smaller error bars (Isern et al. 1998b). The luminosity function of the disk was obtained assuming an age of the disk of 9.2 Gyr and a constant star formation rate per unit volume for the disk, and those of the halo assuming a burst that lasted 0.1 Gyr and started at t_{halo} = 10, 12, 14, 16 and 18 Gyr respectively. Due to their higher cooling rate, O-Ne white dwarfs produce a long tail in the disk luminosity function and a bump (only seen in the cases t_{halo} = 10 and 12 Gyr) in the halo luminosity function. It is important to realize here that the faintest white dwarf known, ESO 439-26, which has a mass M = 1.1-1.2 $M_\odot$ (Ruiz et al. 1995) and a luminosity $\log(L/L_\odot) \sim -5$ is clearly an O-Ne white dwarf and cannot be a halo white dwarf unless the halo stopped its star formation activity less than 8 Gyr ago, since the time necessary for O-Ne white dwarfs to reach this luminosity is at maximum 8 Gyr (García-Berro, Isern, and Hernanz, 1997). In order to make the comparison with observations easier, we display in Figure 6 the same luminosity function in visual magnitudes. The photometric corrections were obtained from the atmospheric tables of Bergeron et al. (1995). Beyond $M_V > 17$ these corrections were obtained by extrapolating from those tables. It is interesting to notice that the distance between the peaks of the halo luminosity functions has increased due to the fact that more and more energy is radiated in the infrared as white dwarfs cool down. Therefore, the detection of such peaks should allow determination of the age of the galactic halo. It is also convenient to remark here that the disk white dwarf luminosity function of Figure 6 was obtained with the same age and normalization factor used for Figure 5, and thus the simulations and the observations are fully consistent.

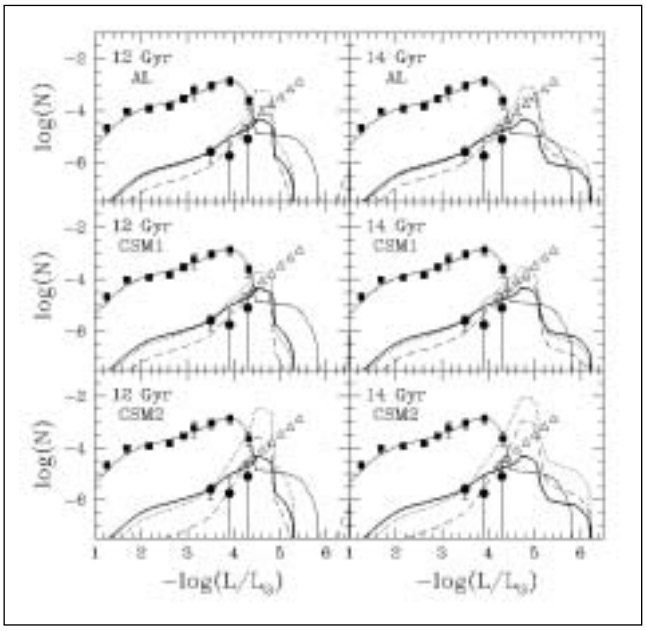

Figure 7. Comparison between the luminosity functions of halo white dwarfs of ages 12 and 14 Gyr and different IMFs (see text for details)

In order to account for the MACHO results in terms of a halo white dwarf population, Adams and Laughlin (1996), and Chabrier et al. (1996) introduced ad-hoc nonstandard initial mass functions that fall very quickly below ~ 1 $M_\odot$ and above ~ 7 $M_\odot$. These functions avoid the overproduction of red dwarfs, the overproduction of heavy elements by the explosion of massive stars (Ryu, Olive and Silk 1990) and the luminosity excess of the haloes of galaxies at large redshift (Charlot and Silk 1995) and, since the formation of very massive and very small stars has been inhibited, the proposed IMFs allow an increase in the number of white dwarfs per unit of astrated mass.

Figure 7 displays the luminosity functions obtained with the IMFs proposed by Adams and Laughlin (1996), with m_c =2.3 and σ = 0.44 – AL case – and the IMFs proposed by Chabrier et al. (1996) – CSM1 and CSM2 cases – for bursts that started 12 (left panel) and 14 (right panel) Gyr ago (dotted lines) and lasted 0.1 Gyr, which we believe are realistic values for the age of the halo, normalized to the brightest and most reliable observational bin. The luminosity function corresponding to the standard case is also displayed for comparison (thick solid line). As expected, the position of the peak does not change but its height increases since the number of main sequence stars below ~ 1 $M_\odot$ is severely depleted. This behavior is due to two different effects: i) The

non-standard IMFs have been built to efficiently produce white dwarfs (0.18, 0.39, 0.53 and 0.44 white dwarfs per unit of astrated mass for the standard, AL, CSM1 and CSM2 cases respectively and for a burst 14 Gyr old, for instance). ii) The time that a white dwarf needs to cool down to the luminosity of the normalization bin, $\log(L/L_\odot) = -3.5$, is ~ 1.8 Gyr and only main sequence stars with masses smaller than 1 $M_\odot$ are able to produce a white dwarf with such a high luminosity if the halo is taken to be older than 12 Gyr. Since the new IMFs have been taylored to reduce the number of stars below ~ 1 $M_\odot$, the luminosity function must be shifted to very high values to fit the normalization criterion. For instance, the values that the different IMFs take at $M = 0.98\ M_\odot$, the mass of the main sequence star that produces a white dwarf with the aforementioned luminosity, are $\Phi_S = 0.23$, $\Phi_{AL} = 0.06$, $\Phi_{CSM1} = 0.2$, and $\Phi_{CSM2} = 0.01$.

Figure 7 also shows that all luminosity functions, except the one obtained from the standard IMF, are well above the detection limit of Liebert et al. (1988) (shown as triangles). This is due to the normalization condition adopted by Isern et al. (1998). If the luminosity function had been normalized to obtain a density of 1.35×10^{-5} white dwarfs per cubic parsec brighter than, $\log(L/L_\odot) = -4.35$ as in Mochkovitch et al. (1990), all the luminosity functions (long dashed in Figure 7) would have been shifted downwards and only those corresponding to the CSM2 case would have remained above the detection limit. Note, however, that except for unrealistic ages of the galactic halo, these IMFs are not only unable to provide an important contribution to the dark matter in the halo, but also to fit the observed bright portion of the luminosity function of halo white dwarfs. For instance, not one of the CSM2 cases appearing in Figure 2 of Chabrier et al. (1996) fits the brightest bin. Therefore a robust determination of the bright portion of the luminosity function could introduce severe constraints to the different allowable IMFs.

7. Conclusions and future prospects

White dwarfs are well studied objects and the physical processes that control their evolution are relatively well understood. In fact most phases of white dwarf evolution can be succesfully characterized as a cooling process. That is, white dwarfs slowly radiate at the expense of the residual thermal energy of their ions. The release of thermal energy lasts for long time scales (of the order of the age of the galactic disk: 10^{10} yr). While their detailed energy budget is still today the subject of some debate, their mechanical structures, which are largely supported by the pressure of the gas of degenerate electrons, are very well modeled except for the outer layers. These layers control the output of energy and a correct modeling is necessary to understand the evolution of white dwarfs.

The sedimentation of chemical species induced by crystallization is one of the major sources of energy of coolest white dwarf stars. The delay introduced by the C/O partial separation is of the order of 1 Gyr (this quantity depends on the model of atmosphere adopted). Minor species present in the white dwarf can also introduce huge delays that can range from 0.5 to 9 Gyr. This uncertainty will be solved when good ternary phase diagrams are available.

White dwarfs can also provide important information about the age of the galactic disk if their luminosity function at low luminosities (especially the cut-off position) is compared with the theoretical predictions. For this purpose it is necessary to have good theoretical models and good observational data. From the observational point of view, the main sources of uncertainty are the distance to the lowest luminosity white dwarfs, the bolometric corrections, and the chemical composition of the outer layers (i.e. DA if hydrogen is present non-DA if hydrogen is absent). At present, the contribution of observational uncertainties to the total error budget of the galactic age can be estimated to be as large as 2 Gyr. Of this amount, 1 Gyr comes directly from the binning and sampling procedure and the statistical noise of the low luminosity bins (García–Berro et al., 1999).

From the observational point of view, the obtention of good luminosity functions of the disk or globular clusters with resolutions in magnitudes better than 0.5 magnitude could easily allow one to test the different phase diagrams. Furthermore, an accurate luminosity function of disk white dwarfs can not only provide a tight constraint to the galactic age and to the shape of the phase diagram of binary mixtures but also has the bonus of providing important information about the temporal variation of the star formation rate.

The scarcity of bright halo white dwarfs and the lack of good kinematical data necessary to distinguish halo white dwarfs from those of the disk have up to now prevented construction of a good luminosity function for the halo (Torres et al., 1998). But probably future missions like GAIA will completely change the situation since high-quality parallaxes and proper motions will result in accurate tangential velocities, thus allowing a good discrimination of these two populations.

Theoretical models indicate that if the halo is not too old, about 12 Gyr, there would be a reasonable chance of detecting the corresponding cut off ($M_V \sim 16$) with surveys as deep as $m_V \sim 20$, provided that the DA specimen were dominant. On the contrary, if non-DA white dwarfs turn out to be dominant, the cut-off would be placed at absolute magnitudes as large as 20 and there would be no chance of detecting it and, thus, of constraining the age of the halo in this way. In any case, indirect information about the halo (age, duration of the burst,...) will come from the comparison of the absolute numbers of red halo dwarfs and white dwarfs in a complete volume limited sample. Furthermore, a robust determination of the bright part of the halo luminosity function could provide important information on the allowed IMFs for the halo and decisively contribute to the solution of the problems posed by the gravitational lensing observations in our halo. Therefore, a simultaneous and self-consistent determination of photometric properties, parallaxes and proper motions of halo white dwarfs could provide us with a unique op-

portunity to set up a solid platform for the study of the halo properties and to set up constraints to its dark matter content.

White dwarfs can be considered as objects well-suited to test any departure from the usual standard physics, since any hypothetical small change can become prominent when the relevant time scales of white dwarf cooling are taken into account. Such is the case, for example, of a hypothetical change in the gravitational constant, *G*. This is due to the extreme sensitivity of the mechanical white dwarf structures to the precise value of *G*. With the invaluable help of the white dwarf luminosity function, an upper bound has been derived (García–Berro et al., 1995) on the rate of change of gravitational constant of $\dot{G}/G \leq -(1 \pm 1) \times 10^{-11}$ yr^{-1}, which is comparable to the bounds derived from the binary pulsar PSR 1913+16 (Damour, Gibbons and Taylor, 1988). Since this is a statistical upper limit, any improvement in our knowledge of the observational white dwarf luminosity function of the galactic disk would eventually translate into a more stringent upper bound.

This is not the only case in which white dwarfs can be used as unique laboratories for fundamental physics. The rate of change of the period of pulsation of several white dwarf variables (DAVs, DBVs and DOVs) can be used to place stringent upper limits on the properties of various weak interacting particles such as axions (Isern et al., 1992), neutrinos (Blinnikov and Dunina-Barkovskaya, 1994) and so on. The key point in this case is very simple: the rate of change of the period of pulsations is well measured for a few variable white dwarfs (G117-B15A is one of the best examples of these non-radial pulsators). The theoretical models predict that the period change rate is directly related to the rate of cooling. Therefore, any additional source or energy sink directly modifies the rate of cooling and, hence, the period's rate of change. Since this rate can be measured with high precision ($\sim 10^{-15}$ s s^{-1}) variable white dwarfs provide us with a unique tool to measure or at least to put bounds to the properties of these exotic particles. This kind of technique can be extended to other particles as well. However, the major drawback of this technique is the poor knowledge of the proper motion, parallax and other fundamental properties of these kinds of pulsators.

Another field in which these non-radial pulsators have been used is the direct determination of the crystallized mass of white dwarfs. More precisely, the size of the crystallized core strongly affects the power spectrum of the non-radial pulsations by introducing a boundary condition: the position of the crystallization front. This front moves with velocities of a few cm/yr. The accurate determination of the position of the crystallization front can at present only be done for BPM 37093 (Winget et al., 1997), a very massive white dwarf. But this places very precise requirements on the crystallization theory. The study of a large enough sample of very massive non-radial pulsators with very wellknown fundamental properties could greatly improve our knowledge of the behaviour of matter at very high densities.

Acknowledgments

This work has been supported by DGICYT grants PB98-1183-C03-02 and PB98-1183-C03-03, by CIRIT grants GRQ94-8001 and PIC98, and by AIHF1997-0087. One of us, EGB, also acknowledges the support received from Sun MicroSystems under the Academic Equipment Grant AEG–7824–990325–SP.

Bibliography

Adams, F., and Laughlin, G., 1996, ApJ, 468, 586
Abrikosov, A.A., 1960, Soviet Phys JETP, 12, 1254
Alcock, C., and Illarionov, A., 1980, ApJ, 235, 534
Alcock, C., Allsman, R.A., Alves, D., Axelrod, T.S., Becker, A.C., Bennett, D.P., Cook, K.H., Freeman, K.C., Griest, K., Guern, J., Lehner, M.J., Mashall, S.L., Peterson, B.A., Pratt, M.R., Quinn, P.J., Rodgers, A.W., Stubbs, C.W., Sutherland, W., and Welch, D.L., 1997, ApJ, 486, 697
Barrat, J.L., Hansen, J.P., and Mochkovitch, R., 1988, A&A, 199, L15
Bergeron, P., Wesemael, F., and Beauchamp, A., 1995, PASP, 107, 1047
Blinnikov, S., and Dunina-Barkovskaya, N., 1994, MNRAS, 266, 289
Caughlan, G.R., Fowler, W.A., Harris, M.J., and Zimmermann, B.A. 1985, Atomic Data and Nuclear Data Tables, 32, 197
Chabrier, G., Ségretain, L., and Méra, D., 1996, ApJ, 468, L21
Charlot, S., and Silk, J. 1995, ApJ, 445, 124
Damour, T., Gibbons, G.W., and Taylor, J.H., 1988, Phys. Rev. Lett., 61, 1151
D'Antona, F., and Mazzitelli, I., 1978, A&A, 66, 453
D'Antona, F., and Mazzitelli, I., 1989, ApJ, 347, 934
D'Antona, F., and Mazzitelli, I., 1990, ARA&A, 28, 139
Díaz-Pinto, A., García-Berro, E., Hernanz, M., Isern, J., and Mochkovitch, R., 1994, A&A, 282, 86
Fleming, T.A., Liebert, J., and Green, R.F., 1986, ApJ, 308, 176
Fontaine, G., and Michaud, G., 1979, ApJ, 231, 826
Figueras, F., García-Berro, E., Torra, J., Jordi, C., Luri, X., Torres, S., and Chen, B., 1999, Balt. Astron., 8, 291
Fontaine, G., Villeneuve, B., Wesemael, F., and Wegner, G., 1984, ApJ, 227, L61
Fontaine, G., and Wesemael, F., 1997 in *White Dwarfs*, Ed.: J. Isern, M. Hernanz and E. García-Berro (Kluwer), p. 173
García-Berro, E., Hernanz, M., Isern, J., and Mochkovitch, R., 1988a, A&A, 193, 141
García-Berro, E., Hernanz, M., Isern, J., and Mochkovitch, R., 1988b, Nature, 333, 642
García-Berro, E., Hernanz, M., Isern, J., and Mochkovitch, R., 1995, MNRAS, 277, 801
García-Berro, E., Hernanz, M., Isern, J., Chabrier, G., Ségretain, L., and Mochkovitch, R., 1996, A&A Suppl., 117, 13
García-Berro, E., Isern, J., and Hernanz, M., 1997, MNRAS, 289, 973

García-Berro, E., Torres, S., Isern, J., and Burkert, A., 1999, MNRAS, 303, 173
Hansen, B.M.S., 1999, ApJ, 520, 680
Hernanz, M., García-Berro, E., Isern, J., Mochkovitch, R., Ségretain, L., and Chabrier, G., 1994, ApJ, 434, 652
Ibata, R.A., Richer, H.B., Gilliland, R.L., and Scott, D., 1999, ApJ, 524, L95
Iben, I., and Tutukov, A.V., 1984, ApJ, 282, 615
Ichimaru, S., Iyetomi, H., and Ogata, S., 1988, ApJ, 334, L17
Isern, J., García-Berro, E., Hernanz, M., and Mochkovitch, R., 1998a, J. Phys.: Condens.
Matter, 10, 11263
Isern, J., García-Berro, E., Hernanz, M., Mochkovitch, R., and Torres, S., 1998b, ApJ, 503, 239
Isern, J., García-Berro, E., Hernanz, M., and Chabrier, G., 2000, ApJ, 528, 397
Isern, J., Hernanz, M., and García-Berro, E., 1992 ApJ, 392, L23
Isern, J., Mochkovitch, R., García-Berro, E., and Hernanz, M., 1991, A&A, 241, L229
Isern, J., Mochkovitch, R., García-Berro, E., and Hernanz, M., 1997, ApJ, 485, 308
Kirshnitz, D.A., 1960, Soviet Phys JETP, 11, 365
Koester, D., and Schönberner, D., 1986, A&A, 154, 125
Kovetz, A., and Shaviv, G., 1976, A&A, 52, 403
Knox, R.A., Hawkins, M.R.S., and Hambly, N.C., 1999, MNRAS, 306, 736
Lamb, D.Q., and Van Horn, H.M., 1975, ApJ, 200, 306
Leggett, S.K., Ruiz, M.T., and Bergeron, P., ApJ, 497, 294
Liebert, J., Dahn, C.C., and Monet, D.G., 1988, ApJ, 332 891
Liebert, J., Dahn, C.C., and Monet, D.G., 1989, in *White Dwarfs*, Eds.: Wegner, G., *IAU Coll. 114*, Springer Verlag, 15
MacDonald, J., Hernanz, M., and José, J., 1998, MNRAS, 296, 523
Méndez, R.A., and Minniti, D., 2000, ApJ, 529, 911
Mestel, L., 1952, MNRAS, 112, 583
Mochkovitch, R., 1983, A&A, 122, 212
Mochkovitch, R., García-Berro, E., Hernanz, M., Isern, J., and Panis, J.F., 1990, A&A, 233, 456
Mochkovitch, R., Isern, J., Hernanz, M., and García-Berro, E., 1997 in *White Dwarfs*, Ed.: J. Isern, M. Hernanz and E. García-Berro (Kluwer), p. 19
Oswalt, T.D., Smith, J.A., Wood, M.A., and Hintzen, P., Nature, 382, 692
Pelletier, C., Fontaine, G., Wesemael, F., Michaud, G., and Wegner, G., 1986, ApJ, 307, 242
Ruiz, M.T., Bergeron, P., Leggett, S.K., and Anguita, C., 1995, ApJ, 455, L159
Ryu, D., Olive, K.A., and Silk, J. 1990, ApJ, 353, 81
Salaris, M., Domínguez, I., García-Berro, E., Hernanz, M., Isern J., and Mochkovitch, R., 1997, ApJ, 486, 413
Salpeter, E.E., 1955, ApJ, 121, 161
Salpeter, E.E., 1961, ApJ, 134, 669
Schatzman, E., 1958, *White Dwarfs*, (Amsterdam: North-Holland)
Ségretain, L., Chabrier, G., Hernanz, M., García-Berro, E., Isern, J., and Mochkovitch, R., 1994, ApJ, 434, 641
Ségretain, L., 1996, A&A, 310, 485
Ségretain, L., and Chabrier, G., 1993, A&A, 271, L13
Shaviv, G., and Kovetz, A., 1976, A&A, 51, 383
Shipman, H., 1997, in *White Dwarfs*, Ed.: J. Isern, M. Hernanz and E. García-Berro (Kluwer), p. 165
Sion, E.M., and Liebert, J., 1977, ApJ, 213, 468
Stevenson, D.J., 1980, J. Physique, 41, C2 – 61
Stevenson, D.J., and Salpeter, E.E., 1976, in *Jupiter*, Ed. T. Gehrels (Univ. Arizona Press), p. 85
Stevenson, D.J., and Salpeter, E.E., 1977, ApJS, 35, 239
Tamanaha, C.M., Silk, J., Wood, M.A., and Winget, D.E., 1990, ApJ, 358, 164
Torres, S., García-Berro, E., and Isern, J., 1998, ApJ, 508, L71
Van Horn, H.M., 1968, ApJ, 151, 227
Vauclair, G., Vauclair, S., and Greenstein, J., 1979, A&A, 80, 79
Weidemann, V., 1968, ARA&A, 6, 351
Winget, D., Kepler, S.O., Kanaan, A., Montgomery, M.H., and Giovannini, O., 1997, ApJ, 487, L191
Wood, M.A., 1995, in *White Dwarfs*, eds. D. Koester and K. Werner (Berlin: Springer), p. 41
Wood, M.A., and Oswalt, T.D., 1998, ApJ, 497, 870
Wood, M.A., Winget, D.E., 1989, in IAU Colloq. 114, *White Dwarfs*, ed. G. Wegner (Berlin: Springer), p. 282
Xu, Z.V., and Van Horn, H.M., 1992, ApJ, 367, 662
Yuan, J.W., 1989, A&A, 224, 108

About the authors

Jordi Isern was born in Llançà (Girona) in 1950. He obtained his doctorate 1978 at the Universitat de Barcelona. He has worked in various universities and research centers such as the Universitat de Barcelona, the Universitat Politècnica de Catalunya and the Instituto de Astrofísica de Andalucía. He is currently Research Professor at the Institut de Ciències de l'Espai in Barcelona.

Enrique García-Berro was born in Jaén in 1959. He obtained his doctorate in 1987 at the Universitat de Barcelona. He has worked at the University of Illinois at Urbana-Champaign. He is currently Associate Professor at the Universitat Politécnica de Catalunya.

Margarida Hernanz was born in Barcelona in 1956. She obtained her doctorate at the Universitat de Barcelona in 1986. She has also worked at the Universitat Politècnica de Catalunya. She is now Research Associate at the Institut de Ciències de l'Espai.

Maurizio Salaris was born in Rome in 1965. He obtained his doctorate in Physics in 1994. He has worked in several research institutes like the Instituto de Astrofísica de Canarias, the Centre d'Estudis Avançats de Blanes and the Max Planck Institute für Astrophysik. He is currently Associate Professor at

the John Moores University of Liverpool.

All of them have done relevant work in several fields of stellar evolution, ranging from the study of red giant stars, Asymptotic Giant Branch stars, novae, supernovae and white dwarfs. In this last field they are considered as leading experts. They have contributed notably to the advance of the physics of the very dense white dwarf interiors.